

Algorithm Theoretical Basis Document

## GCOM-C Evapotranspiration Index Product

Version 1.3

Masahiro Tasumi<sup>1</sup>, Reiji Kimura<sup>2</sup>, Masao Moriyama<sup>3</sup>, Richard G. Allen<sup>4</sup>,  
Ricardo Trezza<sup>4</sup>

<sup>1</sup>Department of Forest and Environmental Sciences, University of Miyazaki  
1-1, Gakuen Kibanadai-Nishi, Miyazaki 889-2192, Japan

<sup>2</sup>Arid Land Research Center, Tottori University

<sup>3</sup>Computer and Information Sciences Program, Nagasaki University

<sup>4</sup>Water Resources Engineering, University of Idaho

March 18, 2016

## Abstract

This Algorithm Theoretical Basis Document (ATBD) describes the algorithm for estimating Evapotranspiration Index (ET<sub>index</sub>) developed as a research product of the GCOM-C satellite of the Japan Aerospace Exploration Agency (JAXA). The ET<sub>index</sub> expresses actual evapotranspiration normalized for the weather condition and is equivalent to the crop coefficient, which has been applied widely for agricultural and irrigation water management around the globe. The ET<sub>index</sub> is convertible to the actual quantity of evapotranspiration by using a local or global weather dataset. The ET<sub>index</sub> is estimated primarily by GCOM-C land surface temperature observation, with some additional inputs including those of a Digital Elevation Model (DEM) and global wind speed data. The final product is a cloud-free 16-day global ET<sub>index</sub> map having a spatial resolution of 250 or 500 m. Daily actual evapotranspiration for any weather condition (including cloud-cover days) is further estimable using a ground-based weather dataset. Additionally, the ET<sub>index</sub> is convertible to volumetric soil water content for locations where information of soil physical characteristics is available.

Employing two extreme hypothetical surface conditions named “wet surface,” defined as a surface having zero sensible heat flux, and “dry surface,” defined as a surface having zero ET, the algorithm estimates ET<sub>index</sub> by using surface temperature as an indicator of surface wetness. The algorithm described in this ATBD has been applied with the MODIS daily land surface temperature map and a global weather dataset. The estimated result was compared with other independent global ET datasets and with some other environmental properties. The comparison implied that the proposed algorithm reasonably estimates ET<sub>index</sub>.

## Table of Contents

1. Introduction.....	1
2. GCOM-C Evapotranspiration Index Estimation Procedure—Overview and Definitions .....	2
2-1. GCOM-C Evapotranspiration Index Map .....	2
2-2. Application of GCOM-C ETindex Product to Soil Moisture Estimation .....	7
3. Algorithm Descriptions.....	8
3-1. Basic Strategy for Estimating Ts(wet) and Ts(dry) .....	8
3-2. Data for Analyses .....	9
3-3. Ts(wet) Estimation.....	11
3-4. Ts(dry) Estimation .....	18
3-5. Calibration for the Maximum Limit of ETindex.....	23
3-6. Adjustments and Filtering of ETindex .....	24
3-7. Calculation of Soil Moisture.....	27
4. Application to Satellite Imagery and Information about Model Accuracy .....	28
4.1. Application Test using MODIS Land Surface Temperature Product .....	28
4.2. Analysis of ETindex for Model Applicability .....	30
4.3. Reality Check of the Estimated Values using Outside Sources.....	31
4.4. Cross-comparisons with Other ET-related Products .....	34
4-5. Discussion and Conclusions .....	36
Acknowledgements .....	37
References.....	38
Appendix: Ts(wet) and Ts(dry) determination model for Shenmu weather measurement site.....	1

## 1. Introduction

Surface evapotranspiration (ET) and near-surface soil moisture are important factors in climate, water balance and circulation, and crop production. The need for satellite-based, global ET estimation has been increasing with the growth of large-scale water and environmental issues, such as global warming, increased instability of weather and climate, water shortages due to population growth, and enhanced human activities. Under these circumstances, the estimation algorithm of the global Evapotranspiration Index (ET<sub>index</sub>) has been investigated as one of the GCOM-C research products. The ET<sub>index</sub> is valuable as an index of evapotranspiration efficiency and soil moisture content. The index is also convertible to the actual amount of ET from the land surface by using a global or local near-surface general weather dataset.

Because the ET<sub>index</sub> is closely related to soil water availability, the information is further convertible to volumetric soil water content ( $\theta$ ), with some additional information of soil physical characteristics, especially that pertaining to the water holding characteristic of soil. Although soil moisture estimation is not the main target of our study for the ET<sub>index</sub> product, this Algorithm Theoretical Basis Document (ATBD) describes the progress toward soil moisture estimation found during the algorithm development work of the ET<sub>index</sub> product.

The first ATBD (version 1.0) was submitted to JAXA in September 2011. The major update from ATBD ver. 1.0 to ver. 1.1 (submitted in March 2013) was the elimination of the elevation function in the estimation of wet-surface temperature. The latitude function was also corrected and modified. The update from ATBD ver. 1.1 to ver. 1.2 (submitted in October 2014) included modification of the ET<sub>index</sub> regulation method and correction of the equations in the Appendix. In this ATBD (version 1.3), description of the theoretical background of the algorithm was improved by including additional information pertaining to the product accuracy. Additionally, the status of soil water content estimation was changed from an additional product to an application output of the ET<sub>index</sub>. No major update from the previous version has been made to the core estimation equations. The development of the ET<sub>index</sub> estimation algorithm is an on-going project. The detailed procedures for ET<sub>index</sub> estimation will continue to be improved, and the ATBD will be updated as necessary.

## 2. GCOM-C Evapotranspiration Index Estimation Procedure—Overview and Definitions

### 2-1. GCOM-C Evapotranspiration Index Map

Evapotranspiration (ET) is controlled by energy and soil water availability along with the near-surface heat and vapor exchange circumstances. The quantity of ET is affected by several factors including weather related factors such as solar radiation, surface and air temperatures, humidity, and wind speed and precipitation, as well as surface topography, land cover, soil type, and status of vegetation. Many of these factors are strongly dependent on region and time, which makes automated global estimation of ET technically difficult. To develop the information infrastructure of global water circulation and consumption, by minimizing the technical difficulty caused by the dependency on region and time, we suggest providing global  $ET_{index}$  via GCOM-C earth observation. The  $ET_{index}$  is ET normalized for the weather condition. The technical difficulty of global ET estimation is mitigated effectively by this normalization.

The GCOM-C  $ET_{index}$  is equivalent to the crop coefficient, which has been applied widely for agricultural and irrigation water management around the globe. The  $ET_{index}$  is defined by the following equation:

$$ET_{index} = \frac{ET_{act}}{ET_0} \quad (1)$$

where  $ET_0$  is reference ET and  $ET_{act}$  is actual ET.

$ET_0$  is typically described as the ET from a well-watered, 12-cm tall grassy field. A detailed definition of  $ET_0$  is the ET from a hypothetical grassy reference field with a crop height of 12 cm, surface resistance of 70 s/m, and albedo of 0.23.  $ET_0$  is calculated using only near-surface weather data (solar radiation, air temperature, humidity, and wind speed). The calculation procedure of  $ET_0$  is described in Allen et al. (1998).

Using the  $ET_{index}$  map and a weather dataset, users can back-calculate actual ET as

$$ET_{act} = ET_{index} \times ET_0 \quad (2)$$

### Framework of the GCOM-C ET<sub>index</sub> Algorithm

In order to achieve a global and near-timely estimation of daily ET<sub>index</sub> with a spatial resolution of 250–500 m, the algorithm should be as simple as possible, with a minimum requirement of input data. In this algorithm, the input data that are used for ET<sub>index</sub> computation are limited to GCOM-C observation data, global DEM data, and near-surface wind speed data.

Our model adopts, from among several types of ET estimation approaches, an estimation approach that produces an index of surface temperature. Kogan (1995) suggested that a surface temperature index having the form of Eq. 3, named the temperature condition index (TCI), can adequately express drought-related vegetation stress:

$$TCI = \frac{Ts(max) - Ts(act)'}{Ts(max) - Ts(min)} \quad (3)$$

where Ts(max) and Ts(min) are the multi-year weekly maximum and minimum surface temperatures, respectively, and Ts(act)' is weekly actual surface temperature (°C).

Kimura (2007) and Senay et al. (2007) proposed indices named the modified temperature/vegetation dryness index (MTVDI) and the ET fraction (ET<sub>f</sub>), respectively. These indices estimate surface evapotranspirative efficiency using the basic structure of a temperature index, as does the TCI, but the timescales of the actual, maximum, and minimum temperatures are instantaneous rather than weekly or multi-annual. In our model, following their findings, the ET<sub>index</sub> is estimated as

$$ET_{index} = C_{adj} \times \frac{Ts(dry) - Ts(act)}{Ts(dry) - Ts(wet)} \quad (4)$$

where Ts(act) is the instantaneous actual surface temperature from satellite thermal

observation ( $^{\circ}\text{C}$ ) and  $T_s(\text{wet})$  and  $T_s(\text{dry})$  are the hypothetical wet surface temperature and the dry surface temperature ( $^{\circ}\text{C}$ ), which are the instantaneous surface temperatures when the surface is expected to have zero sensible heat flux and when the surface is expected to have zero latent heat flux, respectively. The constant  $C_{\text{adj}}$  is an adjustment factor employed in the algorithm.

The constant  $C_{\text{adj}}$  in the equation, representing the maximum limit of the  $\text{ET}_{\text{index}}$  occurring when the surface is in a very wet condition, is uniquely employed in the GCOM-C  $\text{ET}_{\text{index}}$  algorithm. Figure 1 shows an overview of the algorithm for  $\text{ET}_{\text{index}}$  estimation.

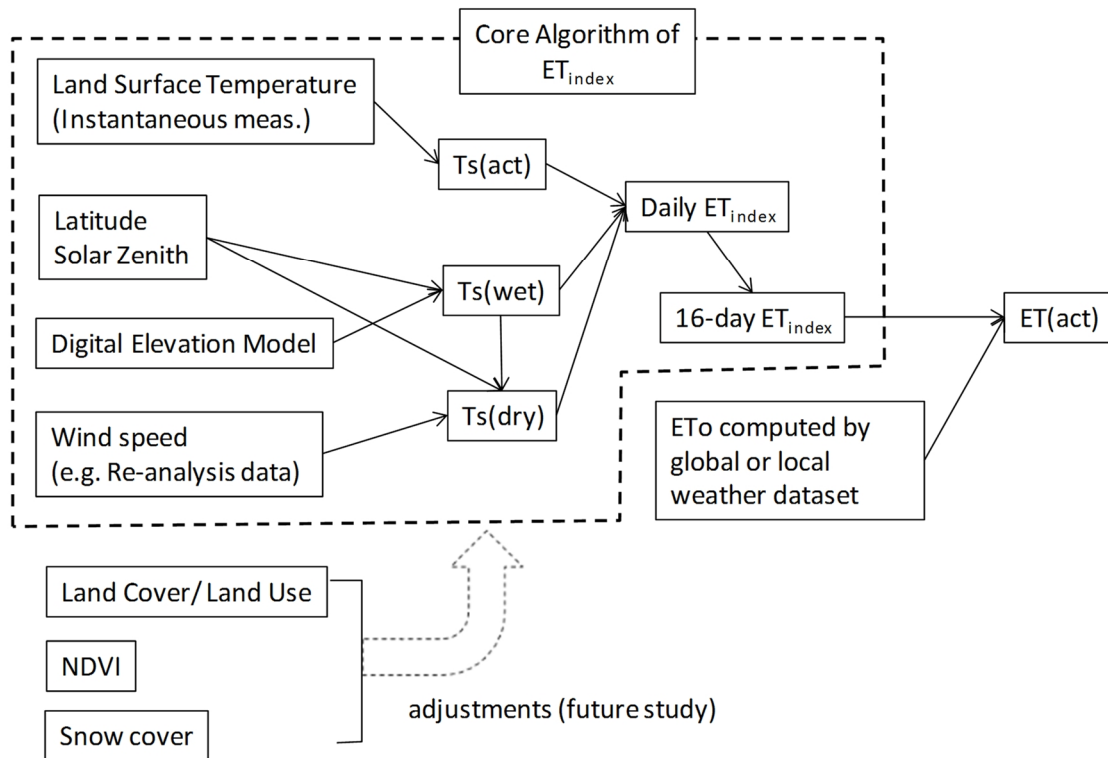


Figure 1. Flowchart of the GCOM-C  $\text{ET}_{\text{index}}$  estimation algorithm.

### Calculation Time Interval

The  $\text{ET}_{\text{index}}$  is first processed on a daily basis, for every day, including cloudy days, using daytime instantaneous land surface temperature (LST) images. The direct estimation of  $\text{ET}_{\text{index}}$  is applicable only for the moment when actual surface temperature is observed by the GCOM-C satellite. For extension of the estimation to a 24-hour

period, we employ an assumption, similar to that of Allen et al. (2007), that the instantaneous  $ET_{\text{index}}$  computed at image time is the same as the 24-hour average  $ET_{\text{index}}$ . GCOM-C will observe the surface every day or two. However, the presence of clouds critically degrades or disables surface temperature observation and thus  $ET_{\text{index}}$  estimation. A small contamination by clouds in a pixel cell, which may be undetectable by an automated cloud-mask algorithm, can cause significant overestimation of  $ET_{\text{index}}$  due to a reduction in the retrieved  $T_s(\text{act})$  value. To automatically prevent the impact of cloud contamination in global  $ET_{\text{index}}$  estimation, daily estimated  $ET_{\text{index}}$  maps are composited every 16 days, and the minimum value of  $ET_{\text{index}}$  over the 16-day period is selected for each pixel as the representative  $ET_{\text{index}}$  value of the 16-day period. However, in some extreme climatic conditions, no single clear-sky day is available within a 16-day composite period. In such cases, because of the cloud effect, the pixel value of the  $ET_{\text{index}}$  automatically takes the maximum number, which may be a good approximation because more than 16 days of continuous cloud is an indicator of the rainy season, during which the surface is expected to be in a wet condition and the  $ET_{\text{index}}$  is expected to take a large number. We accept this assumption for the following reasons:

- (1) Such a condition is expected only in limited areas/seasons of the world.
- (2) Such a condition typically occurs during the rainy season, when the land surface beneath the clouds is in a wet condition and the actual  $ET_{\text{index}}$  value is likely not far from the maximum.
- (3) We want to avoid any data-lacking pixels. Supplying a complete set of 16-day  $ET_{\text{index}}$  maps, with no data-lacking pixels anywhere, is a big advantage. For example, annual ET cannot be estimated if a period lacking data is included.
- (4) In such a cloudy condition with weak solar radiation,  $ET_0$  is expected to be small. Thus, the error in ET is expected to be small even if a somewhat larger error is present in the  $ET_{\text{index}}$ .

The impact of low sensor zenith angle on  $ET_{\text{index}}$  estimation has not been evaluated. However, it will be evaluated after the launch of GCOM-C. In the case that a low sensor zenith angle degrades the estimation of  $ET_{\text{index}}$ , such a pixel might not be used for generation of the 16-day composite image.

#### Application of the Output Data

The GCOM-C  $ET_{\text{index}}$  is applicable to the following purposes:

- (1) Estimate actual ET from GCOM-C ET<sub>index</sub> and weather data.

Users can derive daily, monthly, and annual actual ET maps from the ET<sub>index</sub> map by applying a global or local weather dataset. The required weather data are typically obtainable from any major global weather dataset source or from public weather stations within or near the users' area of interest.

- (2) Use the GCOM-C ET<sub>index</sub> map for relative analyses.

The ET<sub>index</sub> map is a relative indicator of ET. In a specific ET<sub>index</sub> image of an area, pixels having higher ET<sub>index</sub> have higher actual ET. Therefore, the map is usable as is for relative analyses, e.g., identifying areas having higher/lower ET or understanding the yearly trend of ET.

## 2-2. Application of GCOM-C ET<sub>index</sub> Product to Soil Moisture Estimation

The GCOM-C ET<sub>index</sub> essentially indicates the level of soil wetness from zero (very dry) to the maximum (very wet), and it is valuable for estimating soil moisture. The additional input data required to estimate soil moisture are the water holding characteristic of the soil (typically estimated by soil type if directly measured information is not available) and the average root zone depth of the vegetation (if vegetation is present over the surface).

The volumetric soil water content ( $\theta$ ) for the average depth at which the soil water significantly contributes to surface ET can be estimated from the ET<sub>index</sub>. The depth is represented as the root zone if the surface is covered by vegetation or by the top 10–15 cm if the surface is in a bare-soil condition. The volumetric soil water content ( $\text{m}^3/\text{m}^3$ ) is defined by the following equation:

$$\theta = (\text{Volume of soil water})/(\text{Total volume of soil}) \quad (5)$$

Additional and more-detailed information about the soil water estimation procedure using GCOM-C ET<sub>index</sub> is available in Tasumi and Kimura (2013).

### 3. Algorithm Descriptions

Estimation of wet surface temperature ( $T_s(\text{wet})$ ) and dry surface temperature ( $T_s(\text{dry})$ ) is key to the estimation of  $ET_{\text{index}}$ , as shown in Equation 4 and in Figure 1. This section describes the computational algorithms of  $T_s(\text{wet})$  and  $T_s(\text{dry})$ .

#### 3-1. Basic Strategy for Estimating $T_s(\text{wet})$ and $T_s(\text{dry})$

The GCOM-C  $ET_{\text{index}}$  is estimated by indexing surface temperature, which requires two hypothetical surface temperatures, the wet surface temperature ( $T_s(\text{wet})$ ) and the dry surface temperature ( $T_s(\text{dry})$ ).  $T_s(\text{wet})$  is the hypothetical surface temperature assuming that the surface is in a very wet condition. The “wet” surface is defined here as the surface having latent heat equivalent to available energy (i.e., sensible heat is zero).  $T_s(\text{dry})$  is the hypothetical surface temperature assuming that the surface is in a very dry condition. The “dry” surface is defined here as the surface having zero latent heat flux (i.e., zero ET). The definitions of the two extreme surfaces are equivalent to the “cold pixel” and the “hot pixel” of the SEBAL ET estimation algorithm of Bastiaanssen et al. (1998). Whereas the cold and hot pixels of SEBAL are specific pixels of an image, the  $T_s(\text{wet})$  and  $T_s(\text{dry})$  of the GCOM-C  $ET_{\text{index}}$  algorithm are not temperatures of specific pixels but temperatures assigned for every pixel individually.

Theoretically,  $T_s(\text{wet})$  and  $T_s(\text{dry})$  can be determined by solving surface radiation and heat balance (i.e., energy balance) by employing specific assumptions for wet and dry surfaces. However, we have found operational difficulty in obtaining the theoretical solutions of  $T_s(\text{wet})$  and  $T_s(\text{dry})$ . The theoretical approach determines  $T_s(\text{wet})$  and  $T_s(\text{dry})$  by solving energy balance equations to derive long-wave radiation from earth to sky ( $L_{\text{out}}$ ) and then converts  $L_{\text{out}}$  to the hypothetical temperatures. The structural problem of this procedure is that all uncertainties and errors in energy balance computation are cumulated and passed to  $T_s(\text{wet})$  and  $T_s(\text{dry})$ . Therefore, input data quality and robust definition of the hypothetical surface characteristics are critical for successful estimation of the hypothetical temperatures. Because we cannot satisfy these requirements of input data quality and robust definitions of the surface characteristics, using the theoretical approach is operationally difficult. Instead, the GCOM-C  $ET_{\text{index}}$  algorithm takes an empirical approach to determine  $T_s(\text{wet})$  and  $T_s(\text{dry})$ .

### 3-2. Data for Analyses

The development of empirical equations for  $T_s(\text{wet})$  and  $T_s(\text{dry})$  requires near-surface radiation and heat balance measurements. The current version of the algorithm relies largely on micrometeorological data, supplied by Dr. Kimura of Tottori University, measured at Shenmu, China, during 2005 to 2008. The site is located in a part of the Loess Plateau, in a semiarid region of China. Photographs of the weather station and the surrounding area are shown in Figure 2. The data include air temperature, humidity, wind speed and direction, four separated radiation components (solar radiation, reflectance, and longwave radiations from earth and from sky), and soil moisture for 10 different depths. The details of the data measurement are described in Kimura (2007).

Using the weather data,  $T_s(\text{wet})$  and  $T_s(\text{dry})$  were computed by an energy balance model described in the Appendix of this document. An example calculation result for September 9, 2005, is shown in Figure 3.



Figure 2. Photographs of weather station (left) and surrounding area (right) of the Shenmu measurement site ( $38^{\circ}47' \text{ N}$ ,  $110^{\circ}21' \text{ E}$ ; 1224 m a.s.l.).

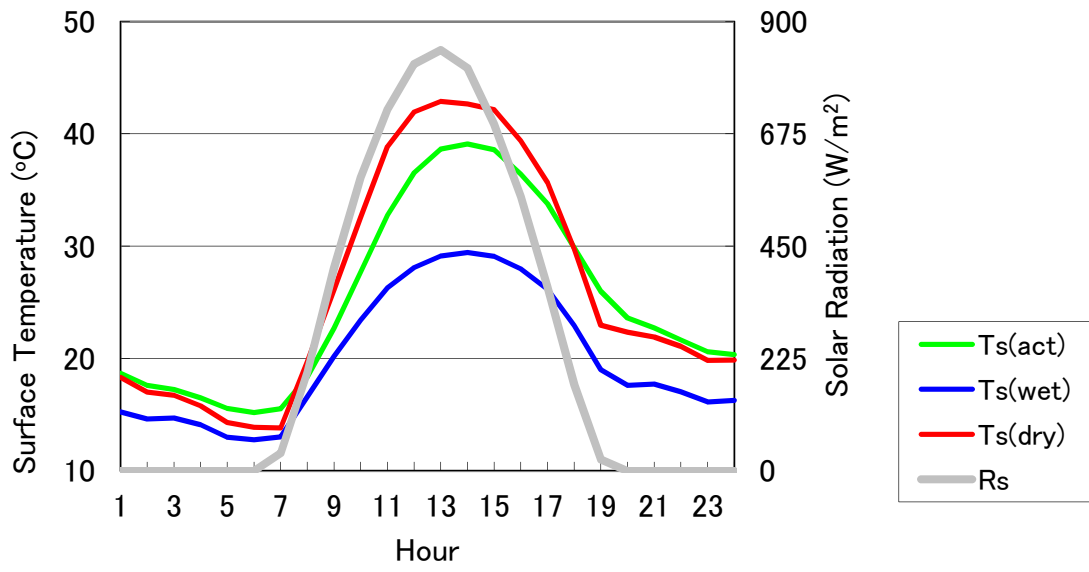


Figure 3. Ts(wet) and Ts(dry) estimated by energy balance computation, plotted with measured actual Ts and Rs at Shenmu, for 9/9/2005.

### 3-3. Ts(wet) Estimation

Wet and dry surface temperatures at 10:30 A.M. on clear-sky days tend to have a linear relationship with radiation, such as solar radiation ( $R_s$ ) or net radiation ( $R_n$ ) (Tasumi, 2010, 2011). Thus,  $T_s(\text{wet})$  and  $T_s(\text{dry})$  are estimated using  $R_s$  or  $R_n$ . Considering the theoretical energy and temperature relationship,  $R_n$  is a more appropriate term to use than  $R_s$ , because  $R_s$  is only one part of the surface radiation balance. Nevertheless, we suggest adopting  $R_s$  to estimate  $T_s(\text{wet})$  and  $T_s(\text{dry})$  because using  $R_n$  results in some operational problems that are difficult to solve.

Considering the global application of the algorithm with GCOM-C satellite measurements, estimating  $R_s$  is much easier than estimating  $R_n$ , because the evaluation of longwave radiation from sky to land surface is difficult. Moreover, the critical problem of using  $R_n$  for  $T_s(\text{wet})$  and  $T_s(\text{dry})$  estimations is the difference between  $R_n$  over an actual surface and  $R_n$  over the hypothetical wet and dry surfaces.  $R_n$  over the hypothetical surfaces is the appropriate term to use to estimate  $T_s(\text{wet})$  and  $T_s(\text{dry})$ . However,  $R_n$  cannot be determined without knowing the hypothetical surface temperatures. Thus, we cannot use  $R_n$  over the hypothetical surfaces for the estimations of hypothetical temperatures. On the other hand, the solar radiation of the hypothetical surfaces is the same as the actual solar radiation. Thus, we can operationally use  $R_s$  for hypothetical surfaces without any problem.

A problem related to the application of actual (not hypothetical)  $R_n$  to estimate  $T_s(\text{wet})$  and  $T_s(\text{dry})$  is visualized in Figure 4. For a certain small area at 10:30 A.M., the spatial difference of net radiation depends on surface temperature and albedo. Hot and bright desert has much lower net radiation than cold forest. If  $T_s(\text{wet})$  is estimated by actual  $R_n$  using an empirical linear regression equation, the estimated  $T_s(\text{wet})$  of desert will be much lower in desert than in forest, which is probably not realistic. If the hot and bright desert is in a very wet condition,  $R_n$  of the surface should be very similar to  $R_n$  of the cold forest, and the  $T_s(\text{wet})$  estimation of the area will be much more homogeneous. This problem is avoided if we use  $R_s$  as the independent variable to estimate the hypothetical surface temperatures.

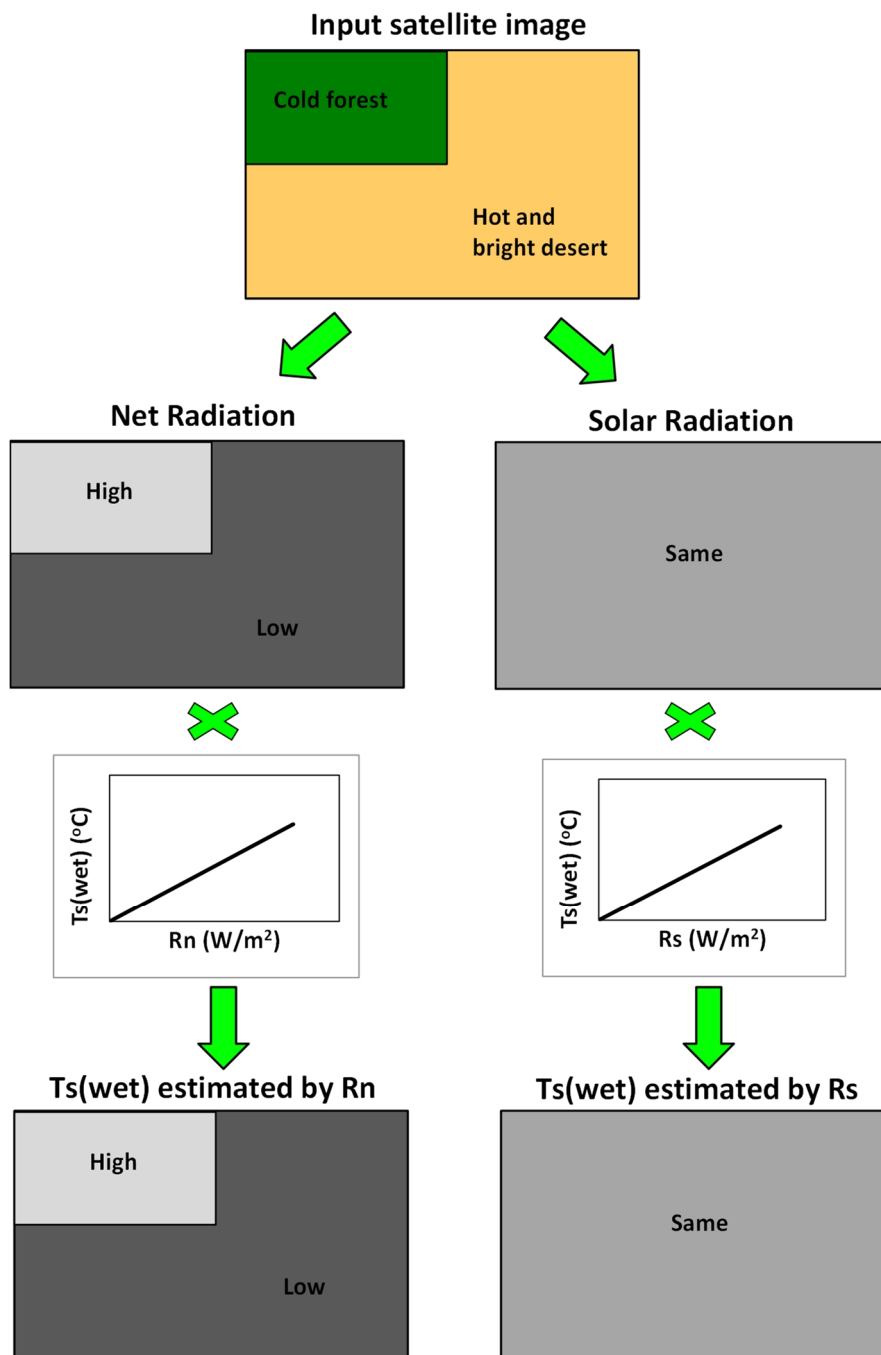


Figure 4. Expected result of  $Ts(wet)$  estimated by net radiation and by solar radiation.

Figure 5 shows the relationship between solar radiation and  $T_s(\text{wet})$  at Shenmu, China, at about 10:30 A.M. (solar time) for clear-sky days during 2005-2008. A clear linear relationship, with large scatter, between  $R_s$  and  $T_s(\text{wet})$  is confirmed. If  $T_s(\text{wet})$  is estimated by the linear regression equation shown in the figure, the standard error of estimation is 7.83 °C, which is large.

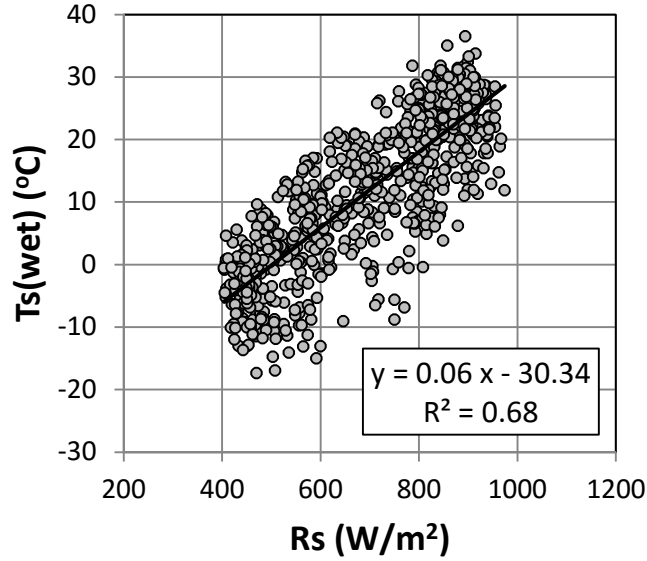


Figure 5. Relationship between measured solar radiation and estimated  $T_s(\text{wet})$  at Shenmu, China, at about 10:30 A.M. (solar time) for clear-sky days during 2005-2008.

The primary reason for the large scatter in Figure 5 is seasonal differences caused by the thermal inertia of the Earth. Figure 6 uses exactly the same data used in Figure 5, but shown as monthly averages. A clear seasonal trend of  $R_s$  and  $T_s(\text{wet})$  is shown, and the trend can be explained theoretically by the thermal inertia of the Earth. In this version of ATBD, the  $R_s$  vs  $T_s(\text{wet})$  relationship with the seasonal trend was expressed as the following equation:

$$T_s(\text{wet}) = 0.06R_s - 30.34 - \sin\left(\frac{\text{DoY} + S_{\text{day}}}{365} \times 2\pi\right) \times f(\text{Lat}) \quad (6)$$

where  $T_s(\text{wet})$  is in °C,  $R_s$  is in  $\text{W}/\text{m}^2$ , DoY is day of year,  $S_{\text{day}}$  is the phase shift of the sine curve calibrated as 37 in the Northern Hemisphere and 220 in the Southern Hemisphere,  $z$  is elevation in meters, and  $f(\text{Lat})$  is the amplitude of the sine curve

determined using latitude (deg.) by  $f(\text{lat}) = -0.0021 \cdot \text{Lat}^2 + 0.3449 \cdot |\text{Lat}| - 2.9864$  ( $0.0 \leq f(\text{lat}) \leq 10.0$ ).

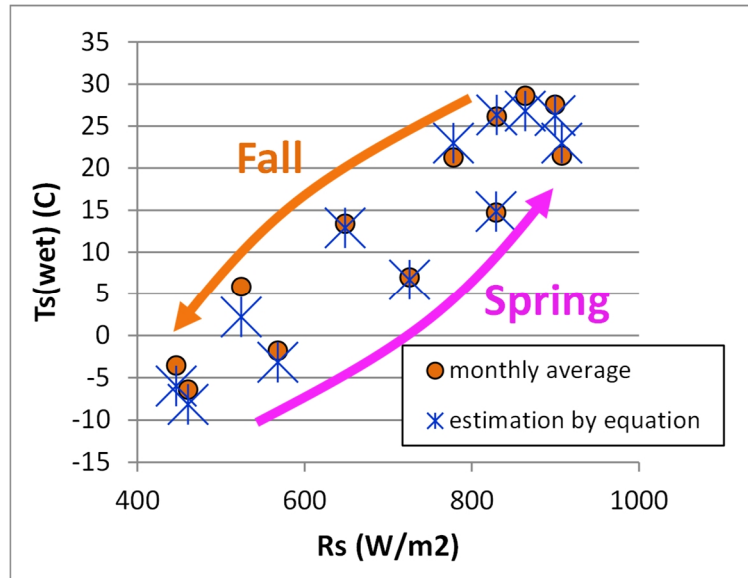


Figure 6. Monthly trend of Rs and Ts(wet) at 10:30 a.m. on clear-sky days along with estimated Ts(wet) from Equation 6.

The first component of Equation 6 “ $0.06R_s - 30.34$ ” is the average linear relationship between Rs and Ts(wet), as shown in Figure 5. The second component of the equation is the sine function describing the seasonal trend between Rs and Ts(wet) calibrated by the Shenmu data (Figure 6). The third component  $f(\text{Lat})$  expresses the amplitude of the sine curve. At Shenmu (latitude =  $38.78^\circ$ ), the amplitude of the sine curve was calibrated as 7.0. If the seasonal trend of the Rs vs Ts(wet) relationship is due to the thermal inertia of the Earth, the amplitude of the sine curve should change with latitude or with the difference of solar radiation that develops the seasons. The seasonal trend would be minimum at the equator and maximum at the location where the difference of solar radiation between summer and winter is largest.

Figure 7 shows the yearly trend of clear-sky solar radiation at 10:30 A.M. by latitude in the Northern Hemisphere. The seasonal difference of solar radiation is smallest near the equator and largest at about  $60^\circ$  latitude. Assuming that the amplitude of the sine curve depends on the difference of solar radiation between summer and winter and assuming that the best value for amplitude at latitude =  $38.78^\circ$  (Shenmu) is 7.0, the amplitude of the sine curve was calibrated as shown in Figure 8.

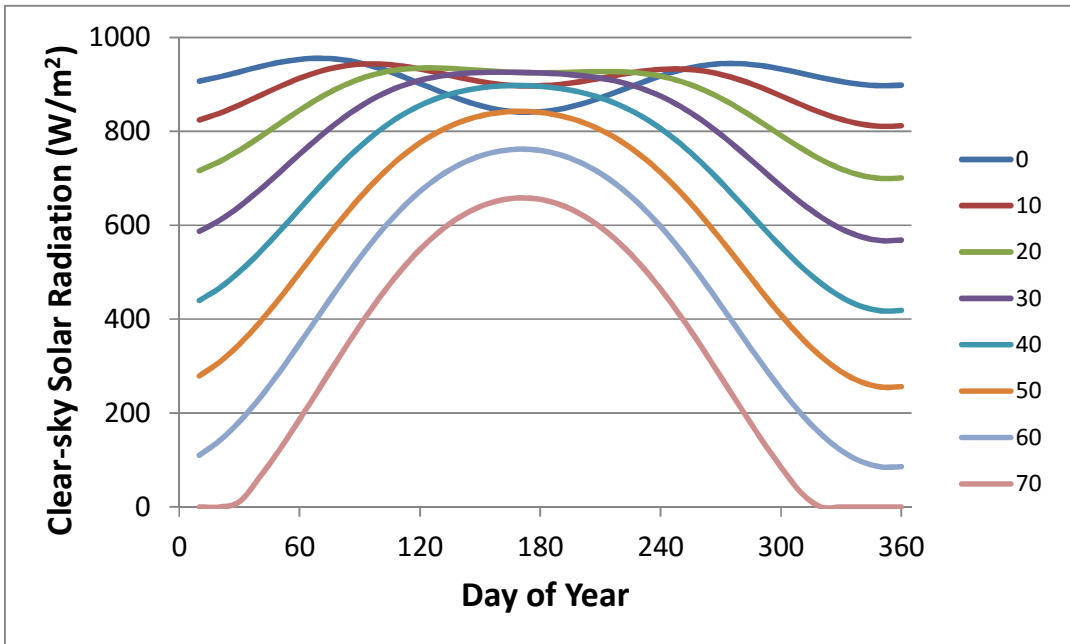


Figure 7. Yearly trend of clear-sky solar radiation at 10:30 A.M. by latitude from 0° to 70° in the Northern Hemisphere calculated assuming the atmospheric condition of the Shenmu measurement site.

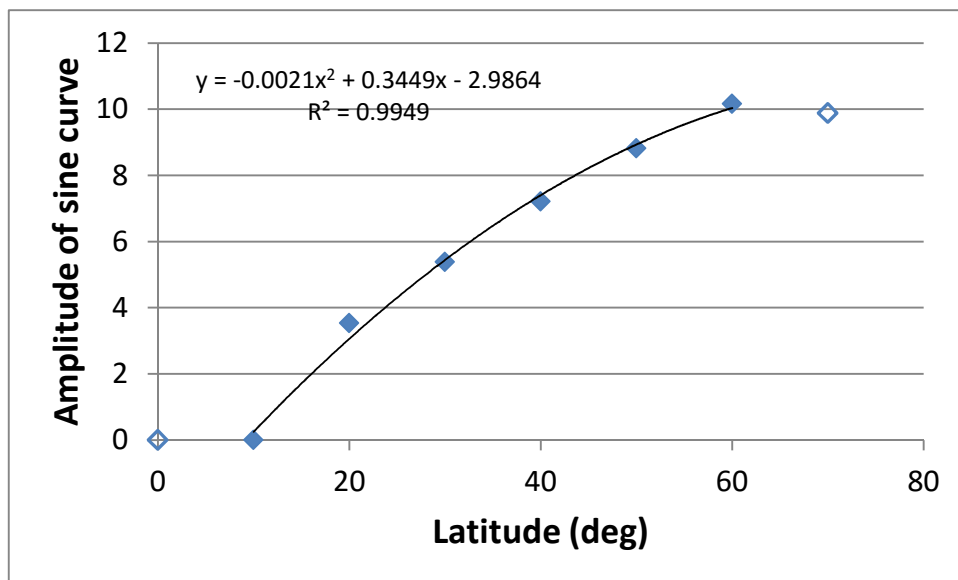


Figure 8. Calibration of the amplitude of the sine curve according to the difference of solar radiation between summer and winter. The amplitudes from 0-10° latitude were set as zero because of no clear winter at these latitudes.

The first version of the ATBD (ver. 1.0) contained an elevation function in Equation 8. However, it was eliminated in the previous ATBD (ver. 1.1) because an analysis indicated that the elevation function was inappropriate (Tasumi, 2013). This version of the ATBD temporarily follows the decision made for version 1.1 for impact of elevation. Future study is required to adequately represent the effect of elevation on  $T_s(\text{wet})$  estimation.

The solar radiation used in Equation 6 is estimated using the solar zenith angle image of the satellite and the DEM. The following equations are based on the clear-sky solar radiation estimation procedure summarized in Allen et al. (1998), organized for application to ETindex estimation. Clear-sky solar radiation is calculated by

$$R_s = \tau \cdot R_a \quad (7)$$

where  $\tau$  is atmospheric transmittance and  $R_a$  is extraterrestrial solar radiation ( $\text{W m}^{-2}$ ).

Atmospheric transmittance is calculated as

$$\tau = 0.75 + 2 \times 10^{-5}z \quad (8)$$

where  $z$  is the elevation (m) given by the DEM.  $R_a$  can be calculated by the following equation:

$$R_a = \frac{G_{sc} \cdot \cos\theta}{d^2} \quad (9)$$

where  $G_{sc}$  is the solar constant of  $1367 \text{ W m}^{-2}$ ,  $\cos\theta$  is the cosine of the solar zenith angle, where the solar zenith angle is supplied as a part of the satellite image, and  $d$  is the relative distance between Earth and Sun calculated as

$$d = \sqrt{\frac{1}{1 + 0.033 \cdot \cos\left(\frac{2\pi}{365} \cdot DoY\right)}} \quad (10)$$

where DoY is day of year.

### 3-4. Ts(dry) Estimation

Compared to wet surface temperature ( $T_s(\text{wet})$ ), dry surface temperature ( $T_s(\text{dry})$ ) is much more sensitive to the micrometeorological condition over the surface (Kanda et al., 2010; Tasumi, 2011). Therefore, direct estimation of  $T_s(\text{dry})$  without sufficient information of the micrometeorology over the surface might entail a considerable uncertainty in estimation accuracy. One operational solution to the problem is to estimate the difference between  $T_s(\text{dry})$  and  $T_s(\text{wet})$  (i.e.,  $T_s(\text{dry-wet})$ ), instead of direct estimation of  $T_s(\text{dry})$ .  $T_s(\text{dry-wet})$  is expected to be more stable than  $T_s(\text{dry})$  for changing micrometeorological condition. After estimating  $T_s(\text{dry-wet})$ ,  $T_s(\text{dry})$  is computed using the following equation:

$$T_s(\text{dry}) = T_s(\text{wet}) + T_s(\text{dry-wet}) \quad (11)$$

The relationship between  $R_s$  and  $T_s(\text{dry-wet})$  at 10:30 A.M. for clear-sky days at Shenmu, China, is shown in Figure 9. The figure clearly shows the impact of wind speed on  $T_s(\text{dry-wet})$ . Within a similar wind speed condition,  $T_s(\text{dry-wet})$  is linearly related to  $R_s$ .  $T_s(\text{dry-wet})$  becomes smaller as wind speed becomes higher. No seasonal trend or effect of thermal inertia was found in the  $T_s(\text{dry-wet})$  vs  $R_s$  relationship, probably because the seasonal impacts available in  $T_s(\text{wet})$  and  $T_s(\text{dry})$  are eliminated when the difference is taken.

The impact of wind speed on  $T_s(\text{dry-wet})$  is explained by Figure 10. This figure shows the relationships between wind speed and the hypothetical surface temperatures for same season (May) for days having similar intensity of solar radiation ( $900\text{--}950 \text{ W m}^{-2}$ ) at 10:30 A.M. for clear-sky days at Shenmu. The graph indicates that higher wind speed decreases the temperatures for both wet surface and dry surface, because wind promotes ET or sensible heat exchange. However, the decrement of surface temperature by wind speed is larger for dry surface than for wet surface, and this is the reason why  $T_s(\text{dry-wet})$  becomes smaller as wind speed becomes higher.

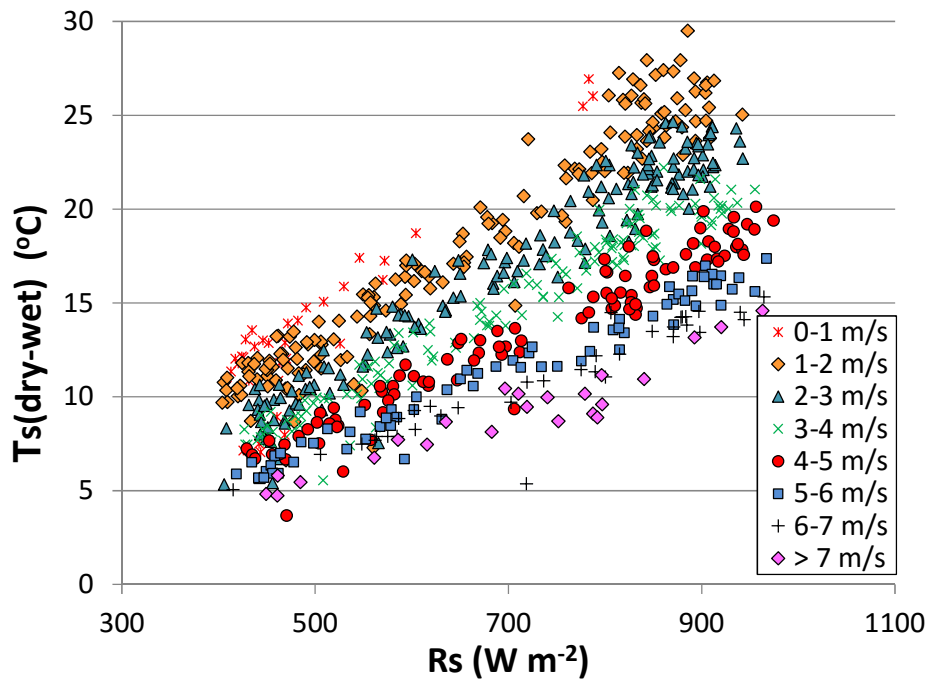


Figure 9. Relationship between measured solar radiation and estimated  $T_s$ (dry-wet) for eight wind speed groups at Shenmu, China, at about 10:30 A.M. (solar time) on clear-sky days during 2005–2008.

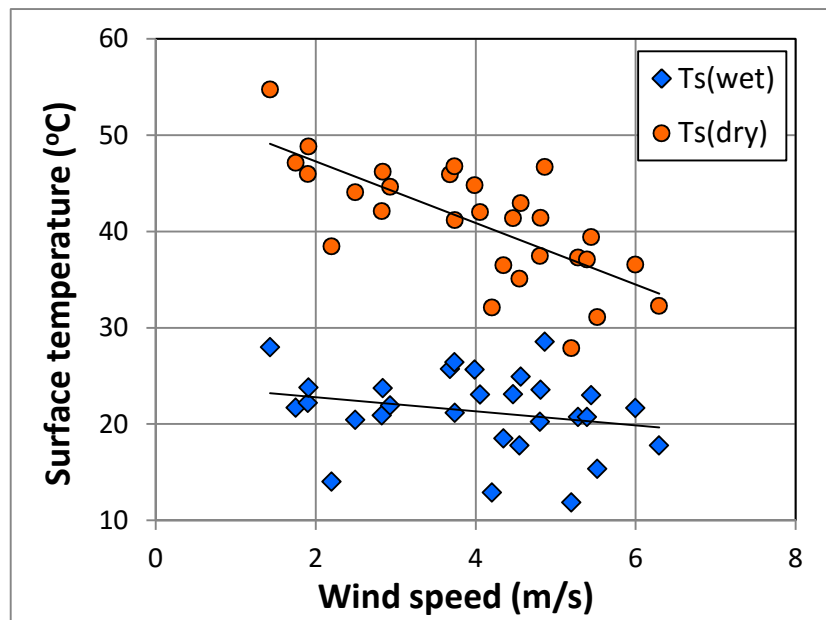


Figure 10. Relationships between wind speed and the hypothetical surface temperatures.

Considering the relations among  $T_s(\text{dry-wet})$ ,  $R_s$ , and wind speed, we propose the  $T_s(\text{dry-wet})$  estimation method summarized in Figure 11. Specifically,  $T_s(\text{dry-wet})$  is proportional to  $R_s$  and the proportional factor changes with wind speed. The proportional factor was calibrated as shown in Figure 12, which uses the data shown in Figure 9. The slopes of the linear regression lines for the wind speed groups in Figure 9 were plotted with the average wind speed of each wind speed group. The resultant equation for  $T_s(\text{dry-wet})$  estimation is the following:

$$T_s(\text{dry-wet}) = (-0.0023u + 0.0301)R_s \quad (T_s(\text{dry-wet}) \geq 0) \quad (12)$$

where  $T_s(\text{dry-wet})$  is in  $^{\circ}\text{C}$ ,  $u$  is wind speed at the height of 2 m in  $\text{m s}^{-1}$ , and  $R_s$  is solar radiation in  $\text{W m}^{-2}$ .

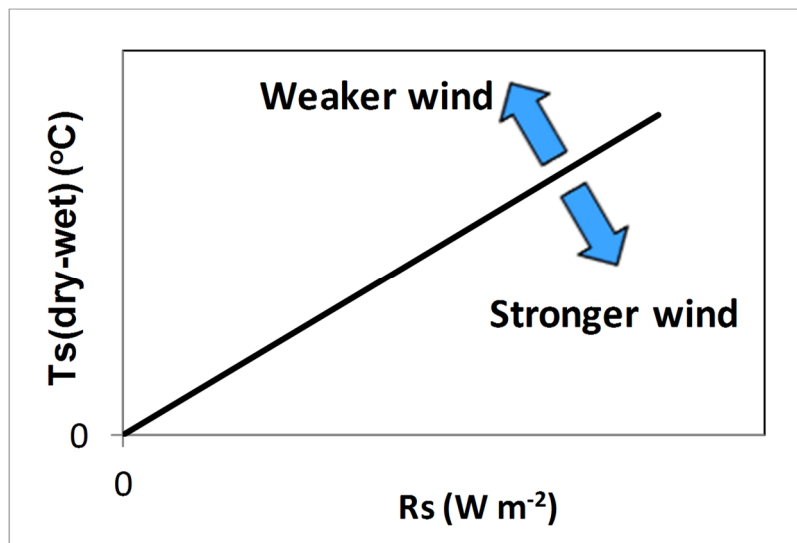


Figure 11. Proposed  $T_s(\text{dry-wet})$  estimation method.

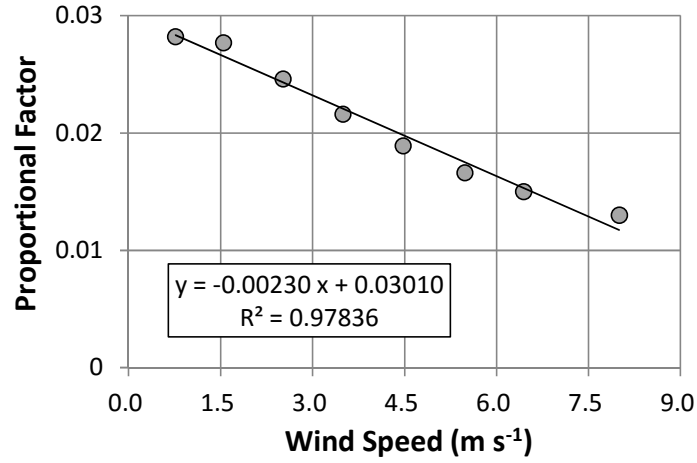


Figure 12. Calibration of the proportional factor.

Equation 12 applies when using wind speed at the height of 2 m. In the case in which the input wind speed data are for a different height, the wind speed data must be converted to wind speed at 2 m using the following equation:

$$u_2 = u_h \frac{\ln\left(\frac{2}{z_{om}}\right)}{\ln\left(\frac{h}{z_{om}}\right)} \quad (13)$$

where  $h$  is the height of the input wind speed data,  $u_h$  is wind speed at height  $h$  (m), and  $z_{om}$  is surface roughness for momentum transport (m).

The  $z_{om}$  is determined using the land cover/land use map. Recommended values of  $z_{om}$  for different land uses, shown in Table 1, were determined by considering the representative values summarized by Kondo (2000).

Table 1. Recommended  $z_{om}$  by land use type.

Land use	$z_{om}$ (m)
Metropolitan	2
Forest	0.6
Town	0.3
Agriculture	0.05
Rangeland	0.05
Water/Snow	$10^{-3}$

### 3-5. Calibration for the Maximum Limit of $ET_{index}$

By definition,  $ET_{index} = 1$  means that the surface has an ET value similar to the one from the hypothetical grassy reference field. The condition of such a surface is different from the “wet” surface determined for  $T_s(wet)$ . Usually, the reference field has positive sensible heat during the satellite overpass time, and therefore the  $ET_{index}$  of the wet surface exceeds 1.0. Namely, the adjustment factor,  $C_{adj}$ , of Equation 4 should exceed 1.0.

The  $C_{adj}$  of Equation 4 was calibrated using Shenmu data. Figure 13 shows a comparison of the latent heat flux from the “reference” surface defined by FAO and from the “wet” surface defined for our  $T_s(wet)$  estimation. The result shows that the ET from the wet surface is 1.23 times greater than the ET from the reference surface if the relationship is assumed to be linear without intercept; however, a non-linear trend was found. The non-linearity indicates that  $C_{adj}$  depends on the intensity of the latent heat flux at the reference or the wet surface, which cannot be determined in this algorithm before determination of  $C_{adj}$ . Therefore, assuming a non-linear relationship, or assuming a linear relationship with intercept in Equation 13, is operationally difficult. In the current version of ATBD, we assume the  $C_{adj}$  of Equation 4 to be 1.23 by adopting a proportional assumption between the reference and the wet surface.

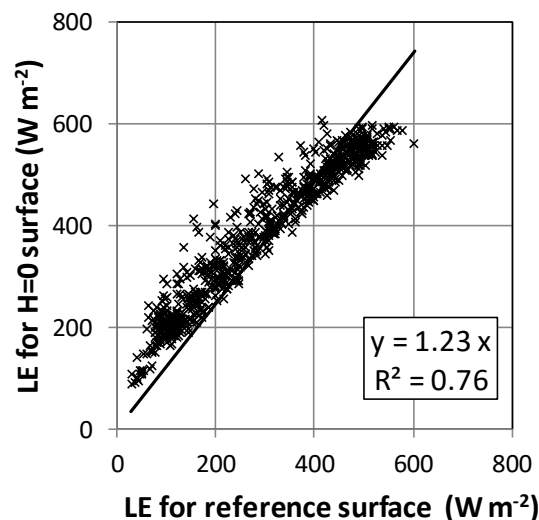


Figure 13. Comparison of latent heat flux from reference surface and from the “wet” surface at about 10:30 A.M. (solar time) for clear-sky days, Shenmu, China.

### 3-6. Adjustments and Filtering of ET<sub>index</sub>

ET<sub>index</sub> expresses the efficiency of ET. It is also strongly related to the soil water content. ET<sub>index</sub> = 0 means that there is no soil water to evapotranspire and that ET is thus zero. ET<sub>index</sub> = 1.23 (i.e., maximum limit) means that sensible heat from the surface is zero at the satellite overpass time (e.g., 10:30 A.M.), which is the wettest condition that the satellite can identify via surface temperature. Thus, the most successful result would be that the calculated ET<sub>index</sub> is between zero and 1.23, without any extra regulation.

However, there is no guarantee that the empirical equations employed in the GCOM-C ET<sub>index</sub> algorithm are applicable to all regions and conditions. To improve the operational accuracy of ET<sub>index</sub> estimation, we suggest additional regulations that might be applicable for the ET<sub>index</sub>. Future studies for model improvement will be conducted to minimize this type of regulation by improving the ET<sub>index</sub> estimation equations themselves.

#### Minimum and Maximum Values of ET<sub>index</sub>

By the definition of dry surface, it is important to limit the minimum value of the ET<sub>index</sub> to zero. The physical meaning of a negative ET<sub>index</sub> is condensation of vapor, which is difficult at a dry surface during the satellite overpass time on clear-sky days. Therefore, a negative value of ET<sub>index</sub> is most likely evidence of underestimation of ET<sub>index</sub>. Additionally, it is effective to limit the maximum value of ET<sub>index</sub> to 1.23, which represents the wet surface condition (H is zero). Theoretically, the actual ET<sub>index</sub> can exceed the ET<sub>index</sub> for the defined wet surface condition in some situations (e.g., in the case of the surface having negative sensible heat at 10:30 A.M. due to, for example, advection of sensible heat). However, setting a maximum number by accepting some underestimation in such rare conditions is a realistic strategy in this type of global application. A global application must target a very wide range of surface, subsurface, and climatic conditions. Also, the data processing should be fully automated. The empirical equations in the algorithm might work poorly in some specific conditions. Thus, setting these minimum and maximum limits of ET<sub>index</sub> can help avoid the occurrence of large error. In this algorithm, ET<sub>index</sub> is limited as

$$0 \leq ET \text{ Index} \leq 1.23 \quad (14)$$

### Regulation of ET<sub>r</sub> Index by NDVI

It is rarely expected that a surface having a high NDVI value (indicating the availability of very active vegetation) would have a very low ET<sub>r</sub> Index value (indicating no or little water to evapotranspire). Adopting this knowledge, regulating the ET<sub>r</sub> Index value by NDVI would improve the estimation accuracy of ET<sub>r</sub> Index.

Figure 14 shows the relationship between NDVI and “ET<sub>r</sub> Fraction” in an agricultural region of the Middle Rio Grande, New Mexico, for 7 satellite images during May to August, 2002. ET<sub>r</sub> Fraction is an index similar to ET<sub>r</sub> Index. NDVI was derived using MODIS Calibrated Radiance with atmospheric correction, and ET<sub>r</sub> Fraction was estimated by the METRIC ET estimation model (Allen et al., 2007) with Landsat imagery, degraded to 500 m (left graph) or 1 km (right graph), supposing the thermal resolution of GCOM-C and MODIS. The only difference between the left and right graph is the spatial resolution of ET<sub>r</sub> Fraction. The gray-colored triangles in the right-bottom part of both graphs are the regions in which ET<sub>r</sub> Fraction cannot be taken, assuming high NDVI and low ET are seldom compatible with each other.

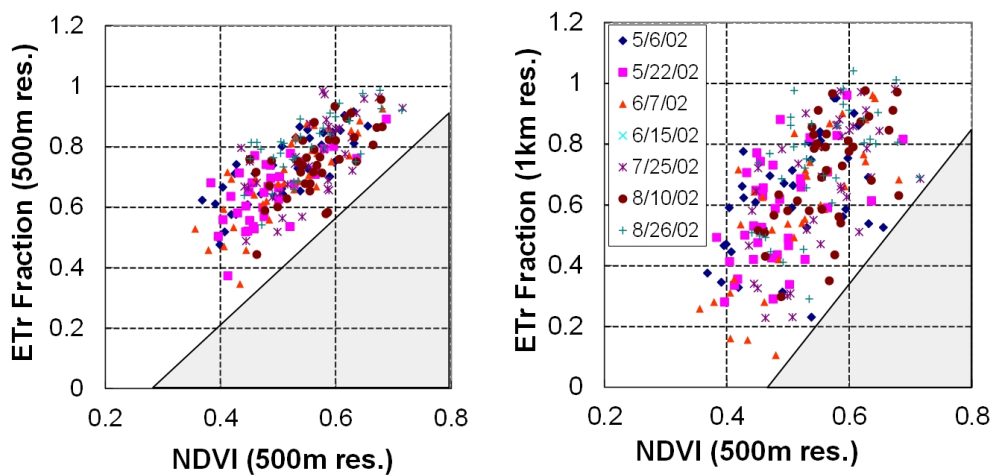


Figure 14. Relationship between NDVI and ET<sub>r</sub> Fraction in an agricultural region of the Middle Rio Grande, New Mexico, for 7 satellite images during May to August 2002. The spatial resolution of the ET<sub>r</sub> Fraction data is 500 m (left graph) and 1 km (right graph).

The graph on the right includes some points having low  $ET_r$  Fraction values at high NDVI values. This is probably due to an inconsistency of footprint between NDVI (500 m resolution) and  $ET_r$  Fraction (1 km resolution). Thus, applying the regulation in the left figure would be more appropriate for our purpose. We temporarily recommend applying the following limitation, in addition to the limitation described in Equation 15, by accepting the result shown in the left-side graph of Figure 14, assuming that the value of  $ET_{index}$  is equivalent to the value of  $ET_r$  Fraction.

$$ET\ Index(min) = 1.80 \times NDVI - 0.54 \quad (15)$$

Equation 15 is only for the suggestion of a framework. The constants in the equation should be re-calibrated using GCOM-C products, with a 250 m resolution basis, after the launch of GCOM-C. The set of constants could be changed by land cover if deemed valuable.

#### Regulation of $ET_{index}$ for Snow/Ice-covered Pixels and for No-sunlight Pixels

On snow/ice surfaces, most of the available energy is expected to be used for melting (i.e., consumed as latent heat of fusion or melting), and thus only a small portion of the available energy is spent on evaporation. Because detection of this very small latent heat is difficult with this type of empirical approach, an operationally reasonable method would be to assign zero  $ET_{index}$  for snow/ice surfaces. This limitation would not induce a large error, especially in the absolute value of  $ET$ , because the available energy itself is generally small on snow/ice surfaces, with their high surface reflectance and small gradient of absolute vapor pressure due to the cold air temperature.

Additionally, some locations on the Earth, typically within the north or south polar circles, may have no solar radiation at 10:30 A.M. This condition violates the application of some of the  $ET_{index}$  estimation equations. For such a surface,  $ET_{index}$  should be assigned as zero. Such a condition occurs in the winter season at high latitude, and the surface is likely to be covered by snow. Again, this limitation would not induce a large error, especially in the absolute value of  $ET$ , because the available energy itself is generally small on snow/ice surfaces, with their high surface reflectance and small gradient of absolute vapor pressure due to the cold air temperature.

### 3-7. Calculation of Soil Moisture

Estimating soil moisture requires information about soil water holding capacity. With this information, one can convert ETindex to soil moisture by adopting the SWEST method summarized in Tasumi and Kimura (2013).

The soil moisture estimation procedure has been tested for a natural grassland condition under semiarid climate using the weather and soil moisture observation data of Shenmu, China. The result indicated that soil moisture was sufficiently estimated at this location (Figure 15). The estimation error of the mean soil water content from zero to 25 cm depth was about 0.029 (i.e., estimation error of soil water was 2.9% of total volume of soil in 1  $\sigma$ ) on average for three years (Tasumi and Kimura, 2013).

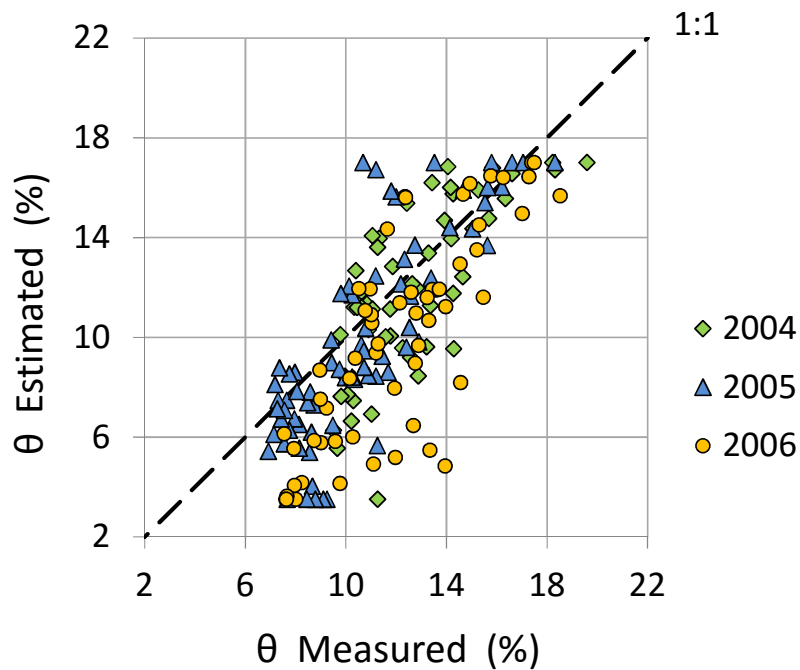


Figure 15. Performance of GCOM-C SM estimation model applied to Shenmu, China, during 2004-2006 (average soil moisture for root zone, 0-25 cm ).

## 4. Application to Satellite Imagery and Information about Model Accuracy

Application tests and accuracy analyses have been made through the past years. The results have been summarized in the yearly report of the project (Tasumi, 2010, 2011, 2012, 2013, 2014, 2015). Some of the results were derived using the older version of the algorithm, and these are not applicable. This section summarizes the currently available information pertaining to model application and accuracy.

### 4.1. Application Test using MODIS Land Surface Temperature Product

The ET<sub>index</sub> was estimated for the entire globe using the MODIS daily surface temperature map for the years 2001–2007 and daily global near-surface wind speed data for the corresponding years supplied by Dr. Mabuchi of Chiba University, Japan. The result of the annual average value for 2001 is shown in Figure 16. Using the daily information, daily ET<sub>index</sub> maps were calculated. The daily maps contained effects of clouds and those had to be eliminated. In this application, the daily maps were grouped into series of 16 days, and the minimum pixel values of the 16-day series were picked up by assuming that the minimum values are the cloud-free, representative ET<sub>index</sub> of the 16 days. For the pixels having no data during the 16 days, the ET<sub>index</sub> value of 1.23 (i.e., the maximum value) was assigned by assuming that such pixels should be wet pixels (16 days of continuous clouds would likely bring some rainfall). No regulation using NDVI or land cover was applied in this application.

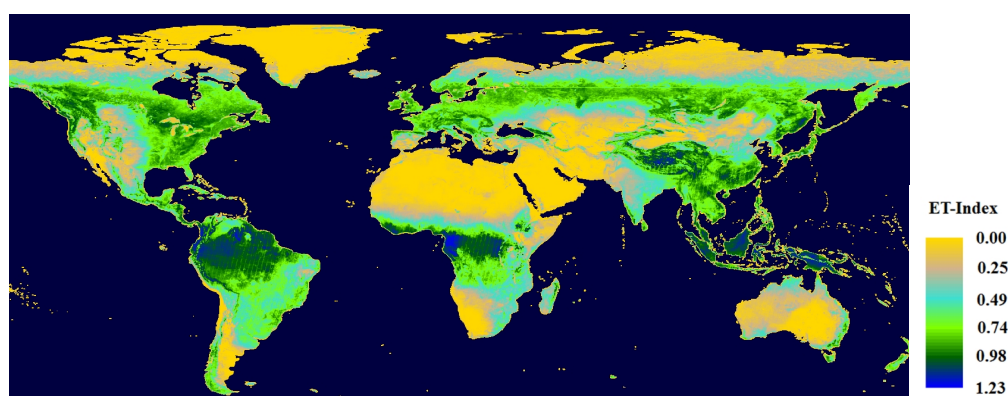


Figure 16. Estimated annual average ET<sub>index</sub> for 2001 from ATBD ver. 1.2.

The 16-day ET<sub>index</sub> was then converted to ET by using additional daily global meteorological data (air temperature, humidity, solar radiation) supplied by Dr.

Mabuchi of Chiba University. The estimation result is shown in Figure 17. In this application, daily ET was calculated by the 16-day ETindex multiplied by the daily ETo, assuming that the ETindex is constant during the 16-day period. This assumption is necessary to avoid the problem caused by cloud cover. Daily ET maps were then accumulated and the annual ET map shown in Figure 17 was derived.

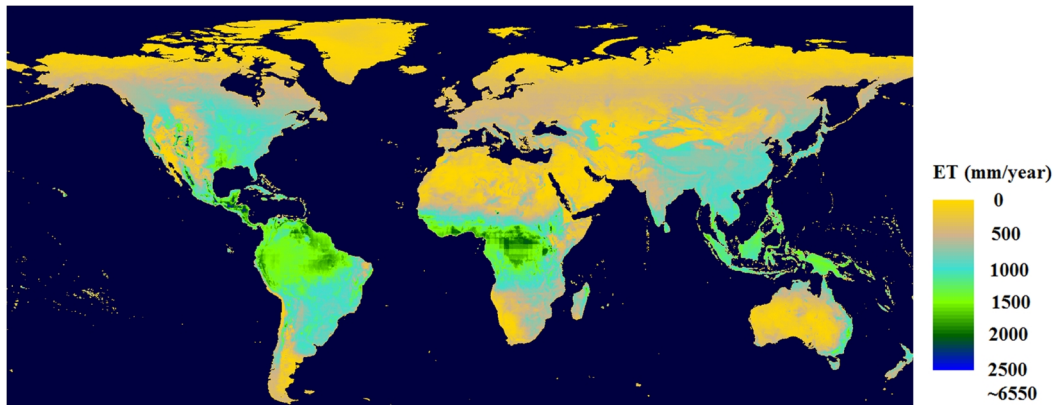


Figure 17. Estimated annual cumulative ET for 2001 from ATBD ver. 1.2.

Note that the annual averaged ETindex shown in Figure 16 is not a simple average of the 16-day ETindex maps. ETindex is calculated using annual ET and annual ETo. In the operational procedure, Figure 16 was derived after Figure 17 was derived. This application test confirmed that operational computation of the algorithm can be conducted without problem.

## 4.2. Analysis of ET<sub>index</sub> for Model Applicability

The proposed ET<sub>index</sub> estimation algorithm has a structure applicable to the entire globe. However, some of the most important equations are empirical equations developed by relying heavily on a location in China. One reasonable method to confirm the adequacy of the estimation algorithm is to calculate the ET<sub>index</sub> value without applying the regulation suggested by Equation 14 and to evaluate the values in “wet” areas of the world. In “wet” areas, the ET<sub>index</sub> is expected to be close to 1.23. If the estimated ET<sub>index</sub> were far above 1.23, or far below 1.23, it would be an obvious indication that our ET<sub>index</sub> estimation has a problem.

Figure 18 shows the seasonal trend of estimated ET<sub>index</sub> for four selected “wet” areas of the world: central Africa, the eastern part of China, central South America, and Southeast Asia. These four “wet” areas were selected manually according to the result of the global application shown in Figure 16. The ET<sub>index</sub> values of each area were averaged values of 20 sample pixels. Ideally, if the surface is in a wet-enough condition, ET<sub>index</sub> reaches 1.23 (but does not exceed 1.23). The result shown in Figure 18 seems to sufficiently meet the criterion. This analysis indicates that the ET<sub>index</sub> estimation is fairly functional, at least in these four selected regions.

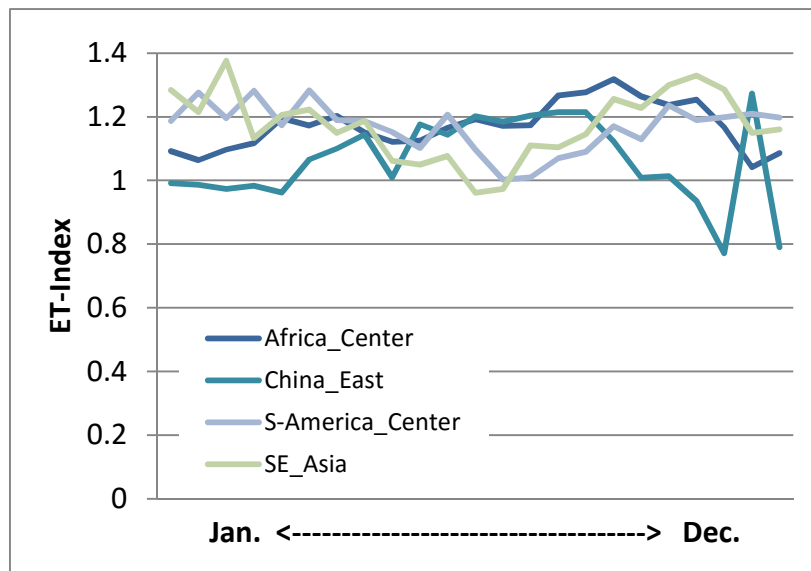


Figure 18. Seasonal trend of estimated ET<sub>index</sub> for four “wet” regions in the world, 2001.

#### 4.3. Reality Check of the Estimated Values using Outside Sources

ET and ETindex are closely related to other types of environmental information, such as climate condition, weather (such as rainfall), vegetation distribution, and so on. A reality check of the estimated ETindex was conducted using the following outside sources.

- (a) Global forest/non-forest map by JAXA (Figure 19)
- (b) Distribution of arid regions map by the Ministry of the Environment (Figure 20)
- (c) Estimated vegetation and precipitation maps of Africa by Sanga and Nonomura (2013) (Figure 21).

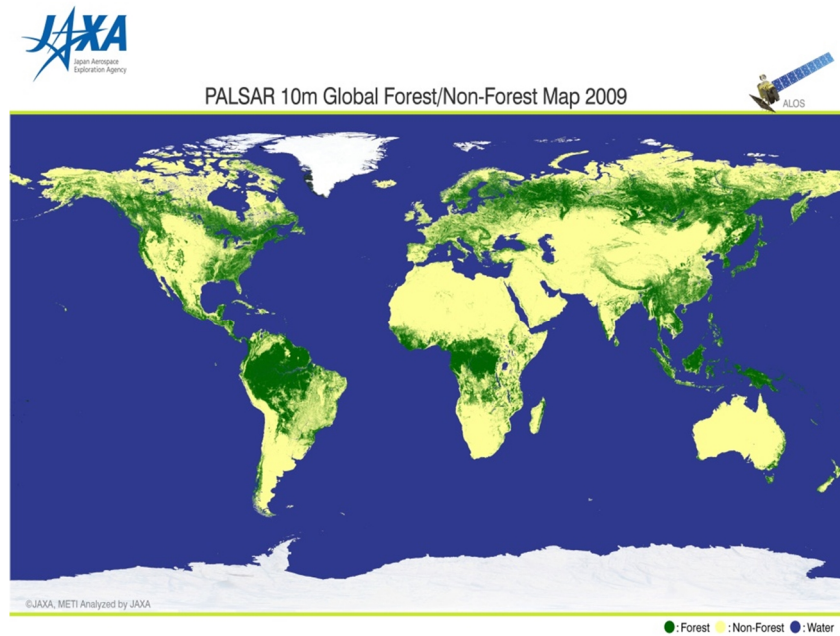


Figure 19. PALSAR 10-m global forest/non-forest map, 2009.

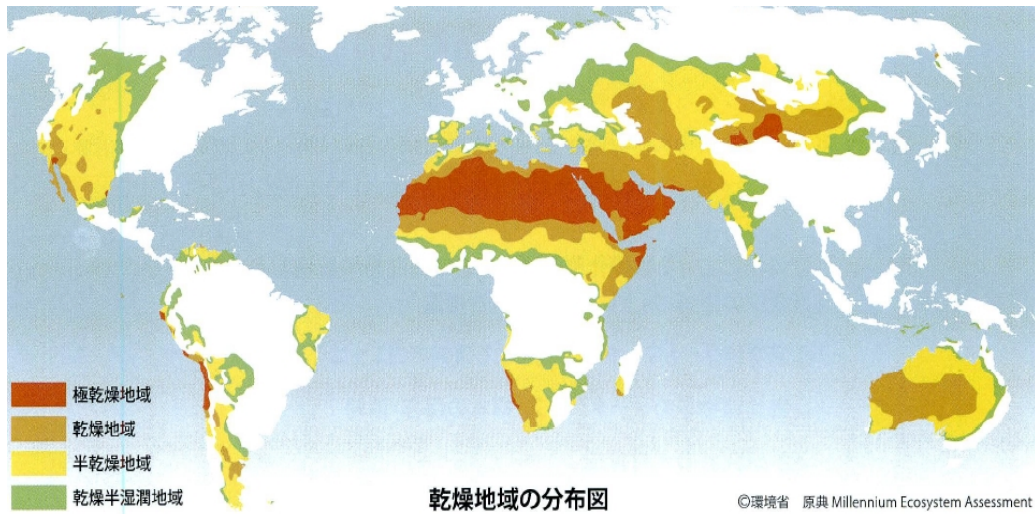


Figure 20. Distribution of arid regions by Ministry of the Environment, Japan.

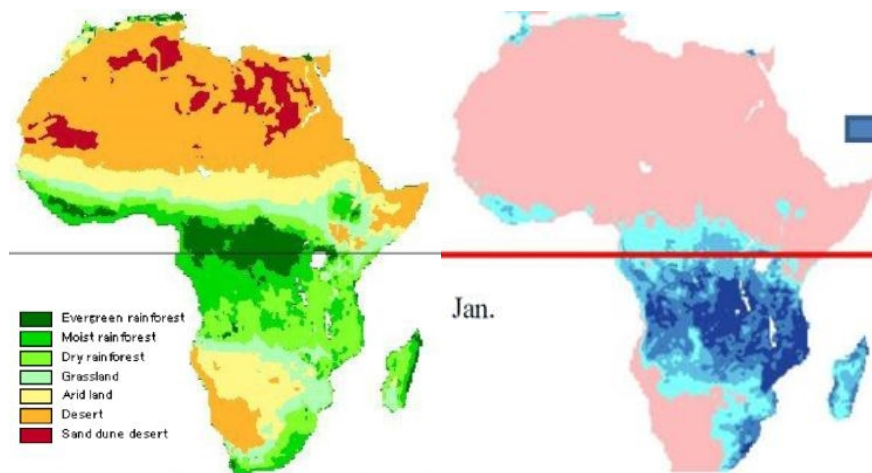


Figure 21. Estimated vegetation (left) and precipitation (right) maps of Africa.

These maps were compared with our estimated results shown in Figure 16. Note that the maps shown in Figures 19-21 are not for the year 2001 but are for different years or for multi-year general information.

The forest distribution (Figure 19) corresponded well with the high  $ET_{index}$  regions of Figure 16, and the distribution of arid regions (Figure 20) corresponded well with the low  $ET_{index}$  regions of Figure 16. The distribution of vegetation on the African continent (Figure 21, left) also corresponded well with the  $ET_{index}$  pattern in Figure 16. Additionally, the monthly precipitation distribution corresponded well with the 16-day estimated  $ET_{index}$  (Figure 22). The results of the comparison indirectly support the adequacy of the  $ET_{index}$  estimation algorithm.

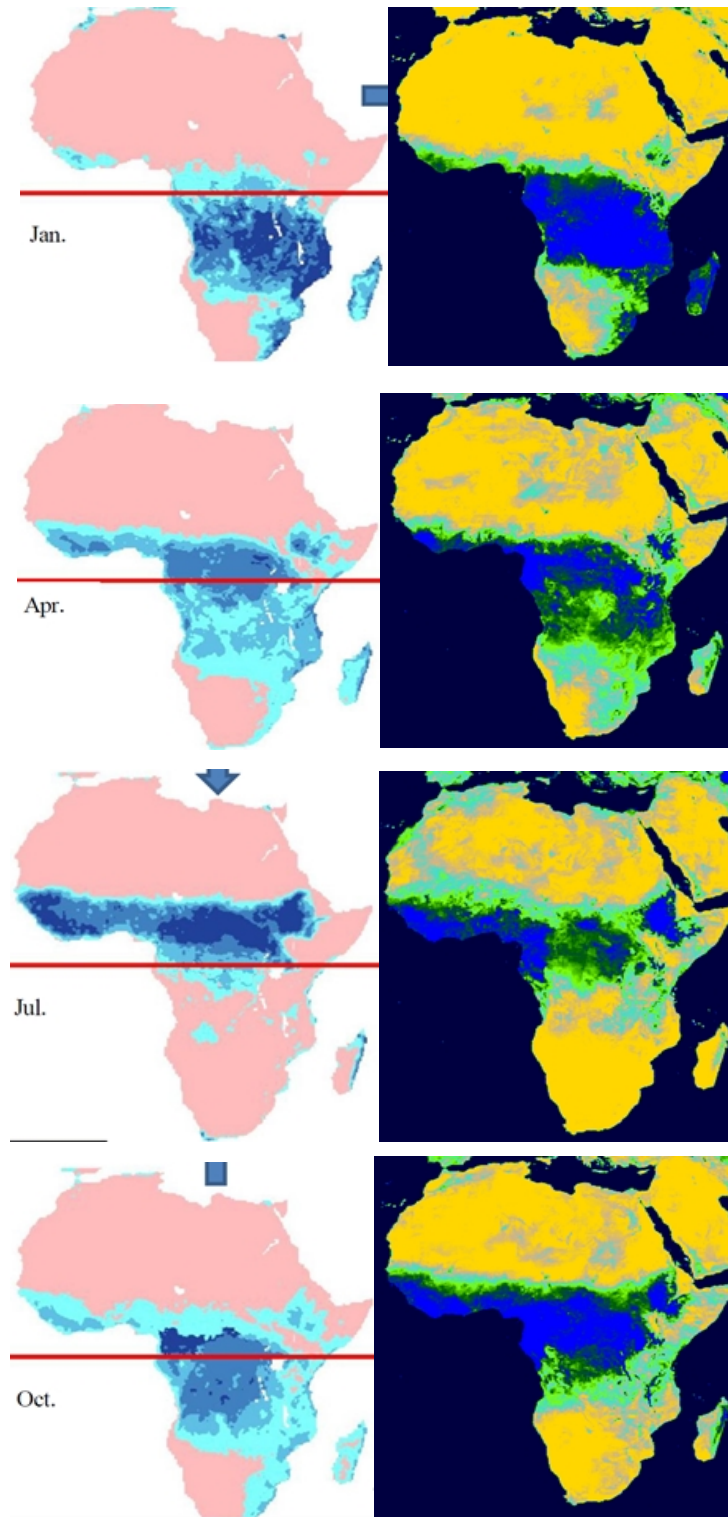


Figure 22. Precipitation distribution in Jan., Apr., Jul., and Oct. compared with corresponding 16-day ETindex maps.

#### 4.4. Cross-comparisons with Other ET-related Products

The estimated ETindex and ET maps were compared with two other types of ET information, the MODIS MOD-16 Global ET product (Mu et al., 2011) and the ET output from a global meteorological model (Mabuchi, 2011). The comparison of ETindex is shown in Figure 23, and the comparison of ET is shown in Figure 24.

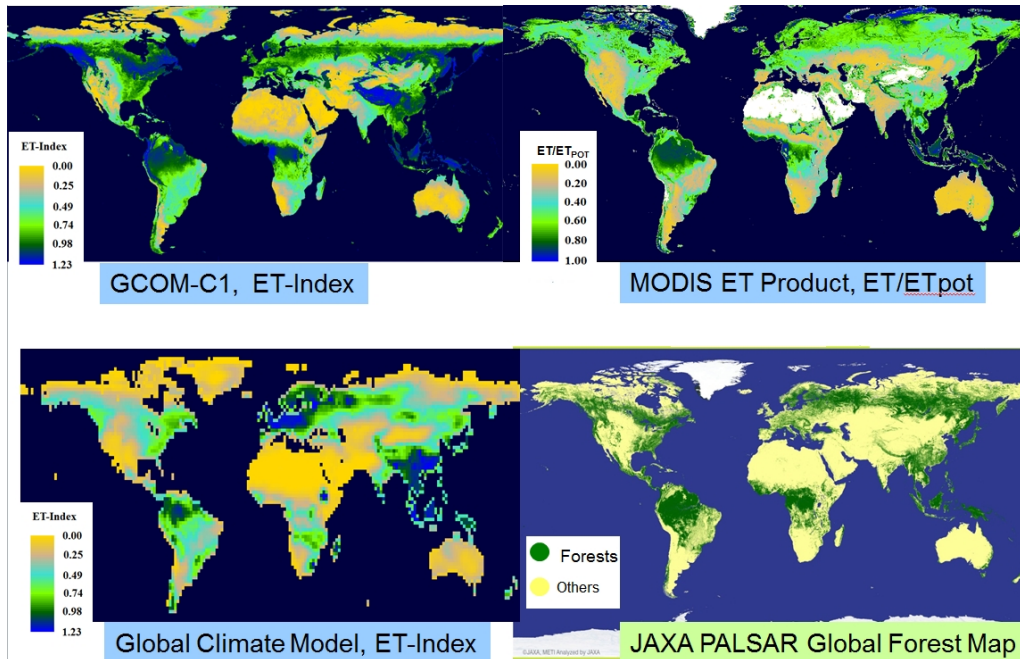


Figure 23. GCOM-C ETindex map compared with the two other ETindex (or ET/ET<sub>pot</sub>) maps, shown with the global forest distribution map. White-colored pixels in the MODIS ET product are data-lacking pixels.

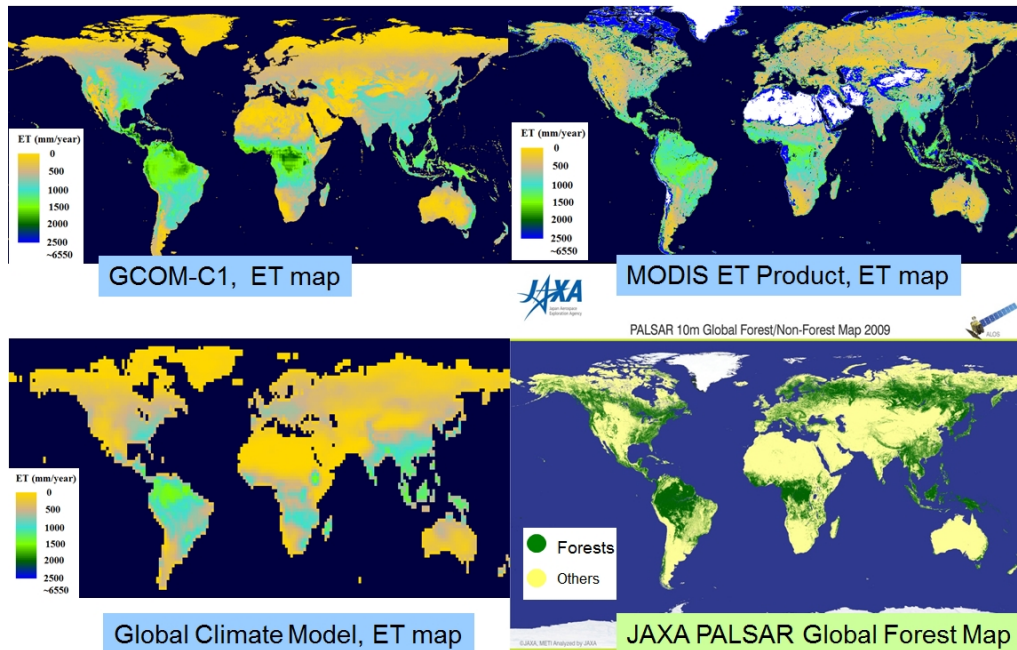


Figure 24. GCOM-C ET map compared with the two other ET maps, shown with the global forest distribution map. White-colored pixels in the MODIS ET product are data-lacking pixels.

The details of the evaluation are discussed in Tasumi (2013). In summary, the GCOM-C ET<sub>index</sub> map agreed fairly well with the other two types of ET map. The ET (and ET<sub>index</sub>) of GCOM-C was higher than that in MOD-16, especially in areas of agriculture. At this point, we consider that the reason for the difference might be underestimation of ET in MOD-16 global ET product. Further evaluation with actual measured ET data is necessary for a more conclusive discussion.

#### 4-5. Discussion and Conclusions

The developed ETindex estimation algorithm was applied to the entire globe using the MODIS daily land surface temperature product and the daily global weather dataset. The proposed algorithm is operationally applicable to the globe with limited input data, and the ETindex is estimated for every pixel, without any data-lacking pixels.

The derived ETindex map was compared with other information, including a forest distribution map, arid region distribution map, vegetation type map, precipitation map, and two other types of ET maps. These comparisons indicated that the spatial distribution of the estimated ETindex was rational.

The current application test does not include the correction/regulation using NDVI and land cover maps, which must be incorporated in the future. Other topics for future study include validation/verification studies using actual ground measurement data.

## Acknowledgements

This research was conducted under the Second and the Fourth Research Announcements of the Global Change Observation Mission (GCOM), funded by the Earth Observation Research Center, Japan Aerospace Exploration Agency (JAXA/EORC). The authors thank Dr. Hiroshi Murakami, Japan Aerospace Exploration Agency, for his continuous support and also thank Ms. Aiko Fujii and other students of the University of Miyazaki for their assistance in this research.

## References

- Allen, R. G., Pereira, L. S., Raes, D., and Smith, M. (1998). "Crop Evapotranspiration." FAO Irrigation and Drainage Paper 56, Food and Agricultural Organization of the United Nations, Rome.
- Allen, R. G., Tasumi, M., Trezza, R., (2007). Satellite-based energy balance for mapping evapotranspiration with internalized calibration (METRIC)—model. *J. Irrig. Drain. Eng. ASCE*. 133.
- Bastiaanssen, W. G. M., M. Menenti, R. A. Feddes, A. A. M. Holtslag, (1998). A remote sensing surface energy balance algorithm for land (SEBAL): 1. Formulation. *J. of Hydr.* 212-213:198-212.
- Junsei K, (2000). *Atmospheric Science near the Ground Surface*. University of Tokyo Press. (in Japanese)
- Kanda, E., Tasumi, M., Ito, F., Ozaki, T., Kimura, R., (2010). 全球蒸発散量推定のための地表面温度指標についての基礎的研究. 2010 年度農業農村工学会講演要旨集.
- Kimura, R., (2007). Estimation of moisture availability over the Liudaogou River Basin of the Loess Plateau using new indices with surface temperature. *Journal of Arid Environments*, 70:237–252.
- Kogan, F. N. (1995). Application of vegetation index and brightness temperature for drought detection. *Adv. Space Res.*, 15, 91-100.
- Mabuchi, K. (2011). A numerical investigation of changes in energy and carbon cycle balance under vegetation transition due to deforestation in the Asian tropical region. *Journal of the Meteorological Society of Japan*, Vol. 89, No.1, pp.47-65.
- Mu, Q., Zhao, M., Running, S. W. 2011. Improvements to a MODIS global terrestrial evapotranspiration algorithm. *Remote Sensing of Environment*. 115:1781-1800.
- Sanga-Ngoie, K., Nonomura, A. 2013. Devising a framework for assessing renewable energy resources in the African biosphere using GIS and remote sensing techniques. 平成 24 年度日本リモートセンシング学会九州支部研究発表会論文要旨集 pp42-44.
- Senay, G. B., Budde, M., Verdin, J. P., Melesse, A. M. (2007). A coupled remote sensing and simplified surface energy balance approach to estimate actual evapotranspiration from irrigated fields. *Sensors*, 7:979-1000.
- Senay, G. B., Budde, M., Verdin, J. P. (2011). Enhancing the Simplified Surface Energy Balance (SSEB) approach for estimating landscape ET: Validation with the METRIC model. *Agricultural Water Management*, 98:606-618.

- Tasumi, M. (2010). 2009 年度宇宙航空研究開発機構共同研究-GCOM 陸圏プロダクトとしての蒸発散指数の開発成果報告書. 宮崎大学.
- Tasumi, M. (2011). 2010 年度宇宙航空研究開発機構共同研究-GCOM 陸圏プロダクトとしての蒸発散指数の開発成果報告書. 宮崎大学.
- Tasumi, M. (2012). 2011 年度宇宙航空研究開発機構共同研究-GCOM 陸圏プロダクトとしての蒸発散指数の開発成果報告書. 宮崎大学.
- Tasumi, M. (2013). 2012 年度宇宙航空研究開発機構共同研究-GCOM 陸圏プロダクトとしての蒸発散指数の開発成果報告書. 宮崎大学.
- Tasumi, M. (2014). 2013 年度宇宙航空研究開発機構共同研究-GCOM 陸圏プロダクトとしての蒸発散指数の開発成果報告書. 宮崎大学.
- Tasumi, M. (2015). 2014 年度宇宙航空研究開発機構共同研究-GCOM 陸圏プロダクトとしての蒸発散指数の開発成果報告書. 宮崎大学.
- Tasumi, M. and Kimura, R. (2013). Estimation of volumetric soil water content over the Liudaogou River Basin of the Loess Plateau using the SWEST method with spatial and temporal variability. *Agricultural Water Management*. 118:22-28.

## Appendix: Ts(wet) and Ts(dry) determination model for Shenmu weather measurement site

This model estimates surface temperatures for hypothetical wet and dry surfaces surrounded by a given weather condition. The wet surface is defined as the surface having no sensible heat, and the dry surface is defined as the surface having no ET. Hypothetical temperatures for the wet and the dry surfaces are named the wet surface temperature (Ts(wet)) and the dry surface temperature (Ts(dry)). The model estimates Ts(wet) and Ts(dry) using surface radiation and energy balance equations with observed ground-based weather data as input data.

Determination of Ts(dry) was made possible by using the energy balance model described below. However, direct determination of Ts(wet) was difficult because of the numerical instability of the iterative computation. To avoid this numerical instability, the surface temperature for a reference surface, Ts(ref), was employed as an initial intermediate parameter prior to estimating Ts(wet).

### Calculation step 1 - determinations of Ts(ref) and Ts(dry)

This model derives Ts(ref) and Ts(dry) from surface energy balance computation. The energy balance equation is expressed as follows:

$$R_n = \ell E + G + H,$$

where  $R_n$  is net radiation ( $W m^{-2}$ ),  $\ell E$  is latent heat flux ( $W m^{-2}$ ),  $G$  is soil heat flux ( $W m^{-2}$ ), and  $H$  is sensible heat flux ( $W m^{-2}$ ).

#### Net radiation ( $R_n$ )

$R_n$  is calculated from the radiation balance equation:

$$R_n = (1 - \alpha)R_s + L_{down} * \varepsilon - L_{up},$$

where  $R_s$  is measured solar radiation ( $W m^{-2}$ ),  $\alpha$  is measured albedo,  $L_{down}$  is measured incoming longwave radiation ( $W m^{-2}$ ),  $L_{up}$  is outgoing longwave radiation ( $W m^{-2}$ ) from

the hypothetical wet or dry surface, and  $\varepsilon$  is surface emissivity (= 0.98).  $L_{up}$  depends on  $Ts(ref)$  and  $Ts(dry)$ .

### Latent heat flux ( $\ell E$ ) and soil heat flux ( $G$ )

$\ell E$  for the wet surface is equivalent to  $ET_o$  by definition.  $ET_o$  is calculated by following the FAO56 equation for hourly data, using surface temperature instead of air temperature:

$$ET_o = \frac{0.408\Delta(Rn - G) \cdot \frac{3600}{10^6} + \gamma \frac{37}{Ts(wet) + 273} u_2 (e_0 - e_a)}{\Delta + \gamma(1 + 0.34u_2)},$$

where  $Rn$  is net radiation ( $W m^{-2}$ ),  $G$  is soil heat flux ( $W m^{-2}$ ),  $Ts(ref)$  is temperature of reference surface (C),  $\Delta$  is saturation slope vapor pressure curve at  $T$  ( $kPa C^{-1}$ ),  $\gamma$  is the psychrometric constant ( $kPa C^{-1}$ ),  $e_0$  is saturation vapor pressure at temperature  $T$  ( $kPa$ ),  $e_a$  is actual vapor pressure ( $kPa$ ),  $u_2$  is wind speed ( $m s^{-1}$ ), and the number  $3600/10^6$  is for the conversion from  $W m^{-2}$  to  $MJ m^{-2} hr^{-1}$ .

$ET_o$  ( $mm hr^{-1}$ ) is converted to latent heat flux ( $W m^{-2}$ ) as

$$\ell E = ET_o * \ell * \frac{10^6}{3600},$$

where  $\ell$  is latent heat of vaporization ( $J kg^{-1}$ ) calculated as

$$\ell = 2.501 - 0.002361 * Ts(wet).$$

$\ell E$  for the dry surface is zero by definition.  $G$  is calculated by the FAO equation as

$$\begin{aligned} G &= 0.1Rn && \text{(for daytime)} \\ G &= 0.5Rn && \text{(for nighttime)}. \end{aligned}$$

In this model, measured albedo is applied when calculating  $Rn$ , which slightly violates the definition of  $ET_o$  (albedo = 0.23). The  $ET_o$  used in this model is a value

adjusted by actual albedo of the site. Also, using measured vapor pressure in ETo estimation might overestimate ETo in the “wet condition” because the vapor pressure over the hypothetical wet surface might be higher than the measured value. This is a limitation of the model.

### Sensible heat flux

Sensible heat flux is calculated by the bulk equation (Kondo, p. 142, Eq. 5.7-5.8):

$$H = C_p \cdot \rho \cdot C_H \cdot u_2 \cdot (T_s - T_a)$$

where  $C_p$  is the heat capacity of air ( $J \text{ kg}^{-1} \text{ K}^{-1}$ ),  $\rho$  is the density of air ( $\text{kg m}^{-3}$ ),  $T_s$  is the hypothetical surface temperature (i.e.,  $T_s(\text{ref})$  or  $T_s(\text{dry})$ ) (C),  $T_a$  is the measured air temperature (C), and  $C_H$  is the bulk coefficient, which is calculated as

$$C_H = \frac{k^2}{\ln(z/z_0)\ln(z/z_T)}$$

where  $k$  is von Karman’s constant (0.41),  $z$  is the reference height (2 m), and  $z_0$  and  $z_T$  are the surface roughness for momentum and heat transfer (m).

During the sensible heat flux computation, an air stability correction was applied via iteration using Monin-Obhukov similarity theory. In this model, measured air temperature was used to estimate  $H$ , which would generate an error on  $H$  estimation of the hypothetical wet and dry surfaces, as the air temperature over the hypothetical surfaces would be different from the measured air temperature. This is a limitation of the model.

### Determination of $T_s(\text{wet})$ and $T_s(\text{dry})$

The optimal solutions for  $T_s(\text{ref})$  and  $T_s(\text{dry})$  are then found by the numerical iteration model. The optimal solutions are the values at which the following equations are valid.

$$(1 - \alpha)Rs + L_{down} \cdot \varepsilon - L_{up} = \ell E + G + H \quad (\text{for reference surface})$$

$$(1 - \alpha)R_s + L_{down} * \varepsilon - L_{up} = G + H \quad (\text{for dry surface})$$

**Calculation step 2 - determination of Ts(wet)**

Ts(wet) is calculated by adjusting Ts(ref) in proportion to the sensible heat:

$$T_s(wet) = T_s(ref) - \frac{T_s(dry) - T_s(ref)}{H(dry) - H(ref)} \times H(ref)$$

The equation is visualized in Figure App.1.

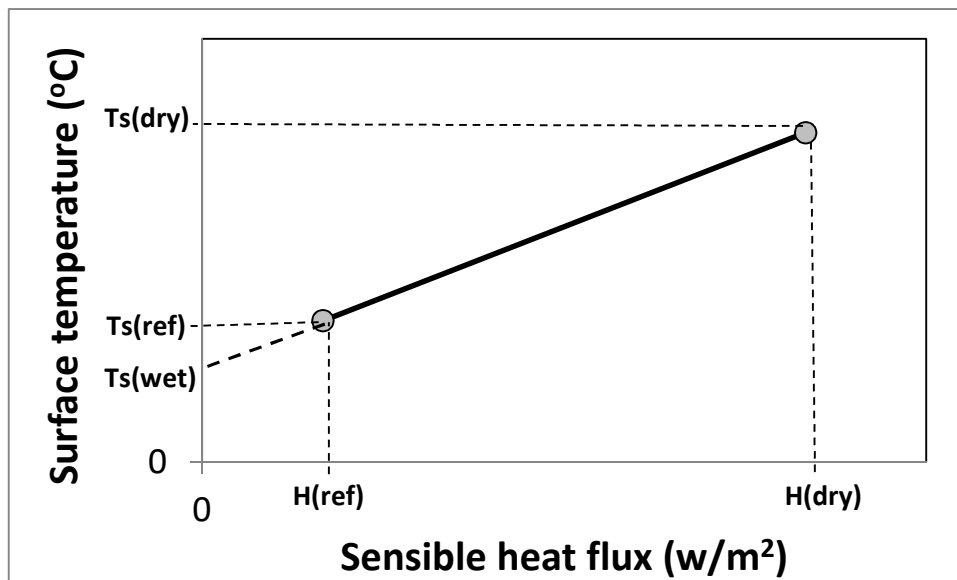


Figure App.1. Ts(wet) determination.